available at www.sciencedirect.com
journal homepage: www.eu-openscience.europeanurology.com

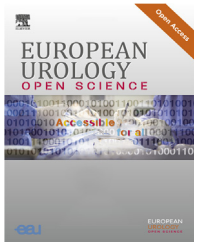

European Association of Urology

Urothelial Cancer

Immune Contexture Changes Following Blue Light Cystoscopy with Hexaminolevulinate in Bladder Cancer

Sara Kaczor Elbæk[a], *Tine Ginnerup Andreasen*[a], *Ann Taber*[a], *Kristine Young-Halvorsen*[b], *Anders Neijber*[b], *Jørgen Bjerggaard Jensen*[a,c], *Lars Dyrskjøt*[a,d,*]

[a] *Department of Clinical Medicine, Aarhus University, Aarhus, Denmark;* [b] *Global Medical Affairs and Clinical Development, Photocure ASA, Oslo, Norway;* [c] *Department of Urology, Aarhus University Hospital, Aarhus, Denmark;* [d] *Department of Molecular Medicine, Aarhus University Hospital, Aarhus, Denmark*

Article info

Article history:
Accepted October 16, 2023

Associate Editor:
M. Carmen Mir

Keywords:
Bladder Cancer
Immune contexture
Blue light cystoscopy
Photodynamic therapy

Abstract

Background: Transurethral resection of bladder tumor (TURBT) is a central component in the diagnosis of non–muscle-invasive bladder cancer (NMIBC) and can be guided by several optical imaging techniques for better visualization of lesions.
Objective: To investigate if a change in tumor microenvironment (TME) composition could be observed as an effect of hexaminolevulinate (HAL)-assisted blue light cystoscopy (BLC) in TURBT samples from patients with bladder cancer.
Design, setting, and participants: This was a retrospective study of 40 patients with bladder cancer who underwent either BLC-guided TURBT (n = 20) or white light cystoscopy (WLC)-guided TURBT (n = 20) before radical cystectomy (RC). Tissue samples (n = 80) were collected from paired TURBT and RC specimens for all 40 patients. Tumor tissue was stained using multiplex immunofluorescence and immunohistochemistry.
Outcome measurements and statistical analysis: Immune cell infiltration was assessed according to the proportions of each immune cell or immune evasion marker and the relative change from TURBT as baseline was calculated. Statistical comparisons between groups were performed using the Wilcoxon rank-sum test or the paired-sample Wilcoxon test.
Results and limitations: Comparison of relative changes in the TME revealed a significant decrease in stromal infiltration of cytotoxic T cells (p = 0.024), B cells (p = 0.041), and stromal cells expressing PD-1 (p = 0.011) in patients treated with BLC-guided TURBT compared to WLC-guided TURBT.
Conclusions: Our pilot study showed that HAL-BLC during TURBT in bladder cancer may influence the immune cell composition and TME.
Patient summary: We investigated the potential therapeutic effect of blue light versus white light for guidance in removing bladder tumors via the urethra in patients with bladder cancer. For blue light guidance, a compound called hexaminolevulinate is

* Corresponding author. Department of Clinical Medicine, Aarhus University, Palle Juul Jensens Boulevard, Aarhus 8200, Denmark. Tel. +45 42271973.
E-mail address: lars@clin.au.dk (L. Dyrskjøt).

https://doi.org/10.1016/j.euros.2023.10.007

used to visualize tumor tissue. We found changes in immune cell composition that may have been influenced by the blue light guidance.

1. Introduction

A significant challenge of traditional white light cystoscopy (WLC) during transurethral resection of bladder tumor (TURBT) is the lack of visibility of certain types of lesions, such as carcinoma in situ (CIS), flat dysplasia (premalignant), and very small tumors. The operating clinician must be able to evaluate suspicious tissue concurrently. It is speculated that incomplete detection of these lesions plays a substantial role in the higher risk of early recurrence often seen in bladder cancer [1]. Different optical techniques are used to aid traditional WLC, including photodynamic diagnosis (PDD). PDD uses light exposure after intravesical instillations of a photosensitizer such as hexaminolevulinate (HAL) [2]. Administration of HAL leads to preferential accumulation of photoactive porphyrins in bladder lesions, which release energy as red fluorescent light upon illumination with a blue light cystoscopy (BLC) system, which helps visualize tumors. Thus, PDD enhances tumor detection and improves complete tumor resection during TURBT. It has been shown that HAL-assisted BLC-TURBT reduces recurrence rates among patients with bladder cancer in comparison to WLC [3–8].

Alongside possible diagnostic value, there is a possible therapeutic effect of other photodynamic procedures, such as 5-aminolevulinic acid (5-ALA) with red light and HAL with white light, in bladder cancer [9,10]. Photodynamic therapy (PDT) is defined as cell death induced by administration of a photosensitizer along with light exposure of a specific wavelength. The mechanism of PDT is complex and not fully elucidated. It is generally believed that the production of reactive oxygen species (ROS) and resulting cell damage are the main mechanisms responsible for the PDT effect; however, other indirect mechanisms of cell death have been proposed, such as inflammatory reactions and vascular damage [11,12]. Cell death followed by local inflammatory reactions could induce an antitumor immune response [11,13]. A plausible hypothesis is that HAL-BLC might induce a PDT-like effect. A recent study using an orthotopic model of bladder cancer in rats demonstrated a treatment effect of HAL-BLC, with evidence of immune activation in terms of tumor infiltration by $CD3^+$ and $CD8^+$ T cells [14]. A change in the tumor microenvironment (TME) may indicate a potential clinical treatment effect beyond pure visualization and detection. The aim of this study was to assess if any measurable change in the TME could be observed in bladder cancer patients as a result of BLC-guided in comparison to WLC-guided TURBT.

2. Patients and methods

2.1. Patients, biological samples, and clinical follow-up

In total, 40 patients with bladder cancer were included in this retrospective study (Supplementary Fig. 1). The following criteria for patient selection were used: (1) primary tumor and subsequent radical cystectomy (RC); (2) no adjuvant therapy, including neoadjuvant chemotherapy, administered between TURBT and RC; and (3) tumor present at the time of RC (pT1–T4a). Formalin-fixed, paraffin-embedded (FFPE) tissue samples (n = 80) from TURBT and RC for all 40 patients were included. In the overall cohort, 20 patients had undergone HAL-BLC-guided TURBT before RC and 20 had undergone WLC-guided TURBT before RC (Fig. 1A). The two patient groups were matched on the basis of tumor stage, grade, treatment history, age, and sex. All clinical information was collected and managed using REDCap electronic data capture tools hosted at Aarhus University. Patients were treated between 2012 and 2020. TURBT was performed at either Aarhus University Hospital or Regional Hospitals in Viborg and Holstebro, Denmark. All RCs were performed at Aarhus University Hospital, Denmark, and patients provided informed written consent to take part in future research projects. The study was approved by The Danish National Committees on Health Research Ethics (#1708266).

2.2. Immunofluorescence, immunohistochemistry, and imaging

Five FFPE sections (3 μm) were stained per patient (Fig. 1B). The tyramide signal amplification strategy was used for multiplex immunofluorescence detection of panel 1 (CD3, CD8, FOXP3) and panel 2 (CD20, CD68, CD163). The strategy we used is similar to that described by Taber et al. [15]. Chromogenic immunohistochemistry was used to detect PD-1, PD-L1, and pan-cytokeratin. Detailed information on the staining protocols and antibodies used is presented in the Supplementary material.

2.3. Digital image analysis

Digital image analysis was performed using the Visiopharm v2020.08.2.8800 image analysis software (Visiopharm A/S, Hørsholm, Denmark). For each tissue section, the fluorescent- or chromogenic-stained image was aligned to its corresponding pan-cytokeratin–stained image. Image analysis protocol packages were developed to (1) define carcinoma and stromal regions of interest (ROIs; Fig. 1C) and (2) identify and quantify positively stained cells. For PD-1 and PD-L1, identification was based on positive brown stains in close proximity to a nucleus. For panels 1 and 2, identification was based on co-localization of selected markers in close proximity to a nucleus (Fig. 1D).

Manual area control was performed on all sample sections to ensure correct alignment and exclude large areas with ulcerations, necrosis, or staining artifacts. Separation of areas with carcinoma cells from stromal areas was based on pan-cytokeratin staining. Only ROIs with a cell count >200 were used for analysis. An intensity threshold was chosen for each marker to separate each fluorophore from the background according to a subjective assessment of the lowest threshold possible for each marker.

Panel 1 and panel 2 stains were aligned to the same section restained for pan-cytokeratin, which allowed direct cell-to-cell alignment and resulted in minimal errors in the alignment process. PD-1 and PD-L1 images (FFPE sections #3 and #5, respectively) were aligned to section #4 stained for pan-cytokeratin. To ensure more precise ROI identification, we created a border ROI, defined as a region between the carcinoma ROI and the stroma ROI. The border had a total width of 28 μm, with 14 μm into the carcinoma ROI and 14 μm into the stromal ROI. The border ROI was discarded, as this comprised potential misalignment and natural variations between, for example, PD-1 and pan-cytokeratin sections (visualized in Supplementary Fig. 2).

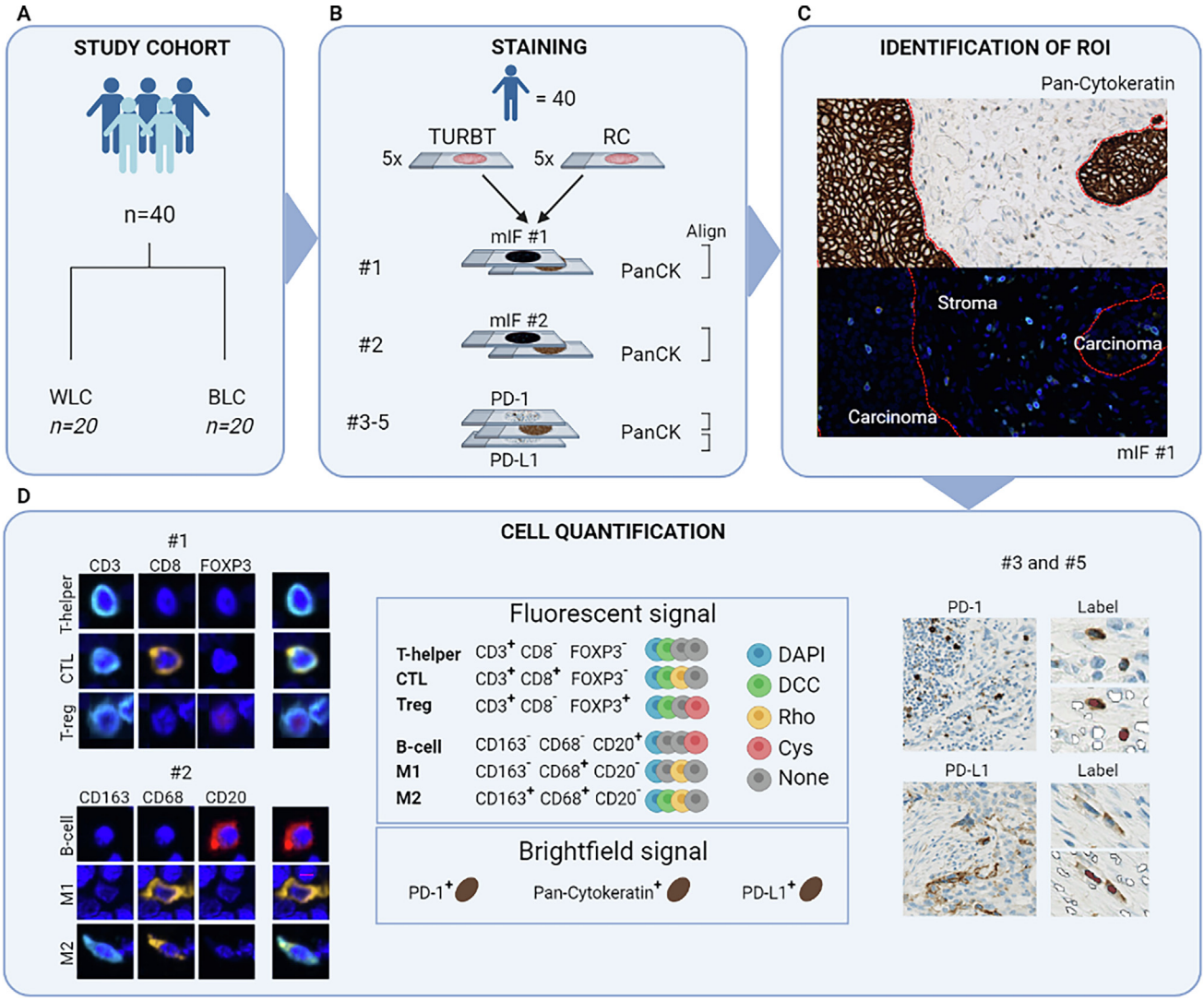

Fig. 1 – Overview of the cohort and study design. (A) Flowchart showing the distribution of the 40 patients in treatment groups. (B) Five serial sections from formalin-fixed, paraffin-embedded tumor specimens were stained and scanned. (C) Digital image analysis was used to identify carcinoma and stroma ROIs on the basis of pan-cytokeratin (A1/A3) staining. Red dashed lines divide tissue into carcinoma and stroma ROIs. (D) Identification of immune cells on the basis of co-localization of selected protein markers (left). Examples of staining results for PD-1 and PD-L1 (right). Cells were quantified within each ROI. WLC = white light cystoscopy; BLC = blue light cystoscopy; TURBT = transurethral resection of bladder tumor; RC; radical cystectomy; mIF = multiplex immunofluorescence; PanCK = pan-cytokeratin (A1/A3); ROI = region of interest; CTL = cytotoxic T cell; Treg = regulatory T cell. Created with Biorender.com.

2.4. Statistical analysis

Statistical comparisons between groups were performed using the Wilcoxon rank-sum test or a paired-sample Wilcoxon test, with p values <0.05 considered significant. Data analysis was performed using R v4.2.2 (RStudio Team) [16].

3. Results

3.1. Clinicopathological data and staining results

To investigate the immune microenvironment in bladder cancer patients treated with WLC-guided or BLC-guided TURBT, we analyzed paired TURBT and RC samples from 20 patients who underwent to WLC-TURBT and 20 who underwent BLC-TURBT. Patient characteristics are summarized in Table 1 and Figure 2 shows representative images of stained tumor samples.

3.2. Changes in the TME between paired samples in the two treatment groups

By comparing paired TURBT and RC samples, we investigated changes in the TME in each treatment group. We sought to explore changes in the proportion (immune cell count/total cell count) of different immune cell types and immune evasion markers from TURBT to RC, stratified by TURBT type. Results for carcinoma ROIs are shown in Figure 3 and for stroma ROIs in Figure 4. We wanted to investigate specifically how immune infiltration changed in the two regions to observe differences between WLC- and BLC-guided TURBT.

In the BLC group, the proportional cytotoxic T-cell (CTL) infiltration in carcinoma regions was significantly higher in RC samples than in TURBT samples ($p = 0.02$). By contrast, in the WLC group the proportional M1 macrophage infiltration was lower in RC samples than in TURBT samples ($p < 0.001$).

Table 1 – Clinicopathological data

Parameter	WLC (n = 20)	BLC (n = 20)	p value[a]
Median time from TURBT to RC, d (IQR)	38 (33–46)	38 (31–48)	0.6
Sex, n (%)			0.3
Female	4 (20)	7 (35)	
Male	16 (80)	13 (65)	
Smoking, n (%)			0.7
Yes	4 (20)	6 (30)	
Former	13 (65)	10 (50)	
No	3 (15)	4 (20)	
Median age at TURBT, yr (IQR)	71 (69–77)	75 (67–76)	>0.9
T stage at TURBT, n (%)			0.057
T1/T1a/T1b	6 (30)	12 (60)	
T2/T2a/T2b	14 (70)	8 (40)	
High grade at TURBT, n (%)	20 (100)	20 (100)	
Carcinoma in situ at TURBT, n (%)	3 (15)	7 (35)	0.14
Histotype at TURBT, n (%)			>0.9
Pure urothelial carcinoma	16 (80)	16 (80)	
Mixed urothelial carcinoma	4 (20)	4 (20)	
T stage at RC, n (%)			0.2
T1/T1a/T1b	3 (15)	7 (35)	
T2/T2a/T2b	5 (25)	8 (40)	
T3/T3a/T3b	9 (45)	3 (15)	
T4/T4a	3 (15)	2 (10)	
High grade at RC, n (%)	20 (100)	20 (100)	
Carcinoma in situ at RC, n (%)	9 (45)	8 (40)	0.7
Histotype at RC, n (%)			0.7
Papillary urothelial carcinoma	0 (0)	1 (5.0)	
Pure urothelial carcinoma	17 (85)	15 (75)	
Mixed urothelial carcinoma	3 (15)	4 (20)	
No tumor	0 (0)	0 (0)	
N stage at RC, n (%)			0.13
N0	13 (65)	18 (90)	
N+	7 (35)	2 (10)	
M stage at RC, n (%)			>0.9
M0	19 (95)	20 (100)	
M+	1 (5.0)	0 (0)	
Recurrence after RC, n (%)	9 (47)	3 (15)	0.029
Unknown	1	0	
Systemic treatment after RC, n (%)[b]	6 (30)	2 (10)	0.2
Survival, n (%)			0.017
Alive	11 (55)	16 (80)	
Died from bladder cancer	9 (45)	2 (10)	
Died from other cause	0 (0)	2 (10)	
Median follow-up, d (IQR)	580 (280–718)	1780 (1529–2634)	<0.001

WLC = white light cystoscopy; BLC = blue light cystoscopy; TURBT = transurethral resection of bladder tumor; RC = radical cystectomy; IQR = interquartile range.

[a] Pearson's χ^2 test, Wilcoxon rank-sum test, or Fisher's exact test, as appropriate.

[b] Patients receiving chemotherapy or immunotherapy (PD-1 or PD-L1 inhibitor) because of recurrence.

Furthermore, carcinoma regions had higher expression of PD-1 at the time of RC than at TURBT in the WLC group (p = 0.02).

The proportions of several immune cell types in the stromal region significantly differed between TURBT and RC in the two treatment groups (T helper cells, regulatory T cells, M1 and M2 macrophages, and cells expressing PD-L1). The proportions of these four cell types and cells expressing PD-L1 were lower in RC samples than in TURBT samples in both groups. Interestingly, differences in B cells and cells expressing PD-1 were significant in only one of the patient groups. The proportion of stromal B cells was significantly lower in RC samples than in TURBT samples in the BLC group (p = 0.04) but not in the WLC group (p = 0.6). We observed a decrease in stromal PD-1 expression in patients who underwent BLC-guided TURBT (p = 0.005).

3.3. *TME differences between patient groups*

We compared changes in immune cell infiltration and immune evasion markers between WLC-guided and BLC-guided TURBT. The immune cell fraction in the TURBT sample was defined as the baseline and the change was calculated relative to this (Fig. 5).

Comparison of the relative changes in the TME, we found no significant difference between the WLC-guided and BLC-guided TURBT groups for carcinoma regions. However, we observed significantly lower stromal infiltration by CTLs (p = 0.024), B cells (p = 0.041), and cells expressing PD-1 (p = 0.011) in the BLC group than in the WLC group.

4. Discussion

We evaluated immune cell infiltration and immune evasion markers in bladder tumors and the surrounding stromal environment following BLC-guided TURBT to investigate the change in immune contexture as a possible therapeutic mechanism underlying the long-term clinical effect seen after BLC-guided TURBT.

The fraction of several immune cells and immune evasion markers significantly differed between TURBT and RC in the two treatment groups, which may be because of differences in the tissue composition of the two sample types. In general, we detected a decrease in immune cells in the stromal region, which may be explained by the difference in size of tissue available from TURBT and RC samples. The TURBT samples were considerably smaller in stromal region size in comparison to RC samples, in which the stromal region was composed of large areas of muscle and adipose tissue with a lower amount of immune cells. This could result in lower stromal immune-cell fractions in RC samples than in TURBT samples. Consequently, to compensate for differences in tissue composition between TURBT and RC samples, we calculated the relative change in immune cell infiltration to obtain a more reliable relative comparison between BLC-TURBT and WLC-TURBT.

Comparison of the relative change in stromal immune-cell infiltration between the treatments revealed significantly lower CTL infiltration in BLC-TURBT than in WLC-TURBT samples. Comparison of paired TURBT and RC samples from patients treated with BLC-TURBT revealed a significant increase in CTLs in carcinoma regions and a trend towards a decrease in CTLs in stromal regions. This indicates that BLC-TURBT treatment has a greater effect on CTL infiltration than WLC-TURBT does. CTLs play a central role in antitumor immunity [17]. Lamy et al. [14] used an orthotopic model of bladder cancer in rats to investigate immune cell infiltration in rats receiving HAL-assisted BLC. They observed an anti-tumor effect and an indication of immune activation following HAL-BLC according to visual assessment of immunological markers ($CD3^+$, $CD8^+$, and $CD4^+$), with observation of intratumoral $CD3^+$ and $CD8^+$ immune

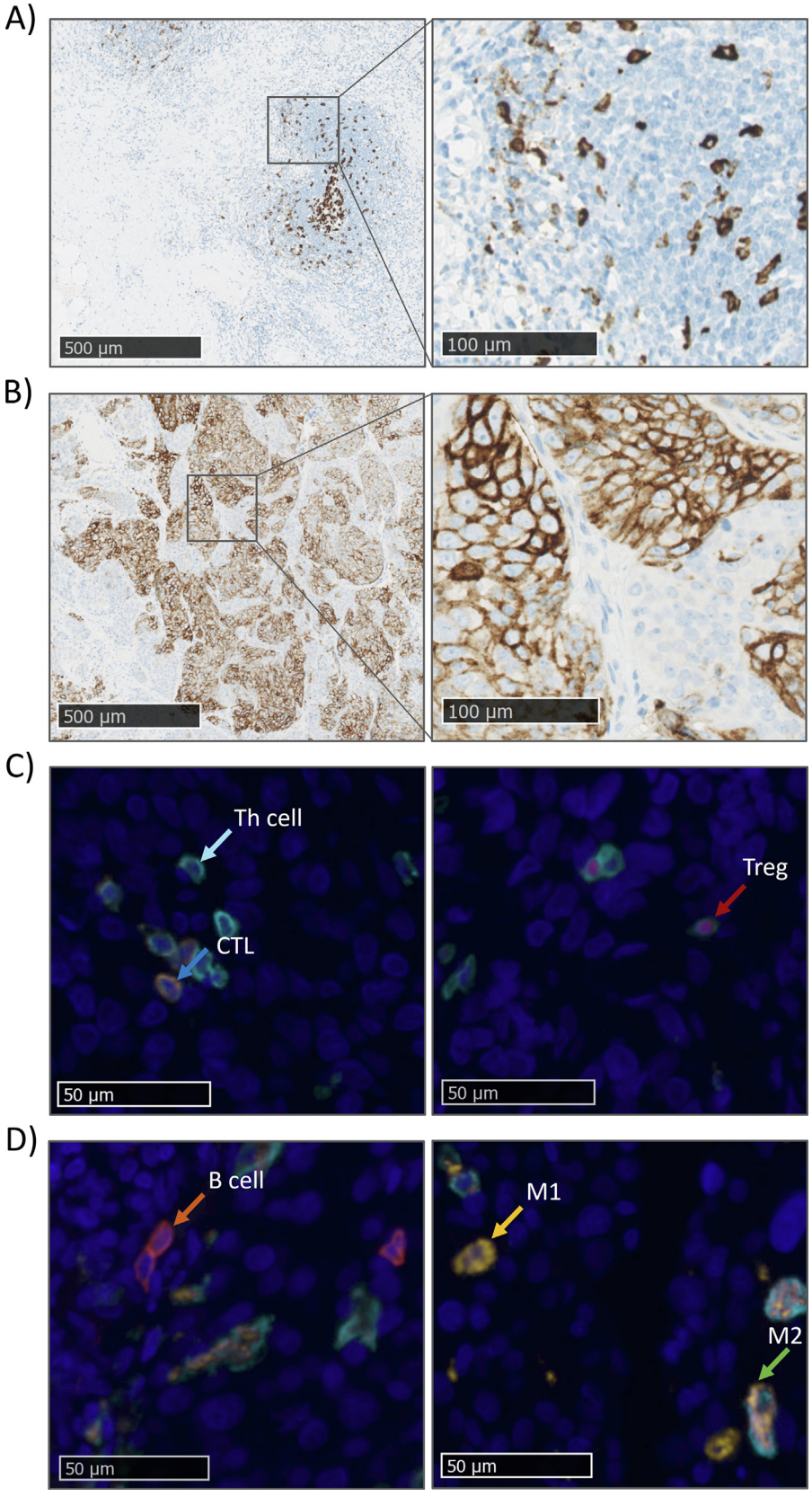

Fig. 2 – Representative images of tumor samples stained for PD-1 and PD-L1 expression and T helper (Th) cells, CTLs, Tregs, B cells, M1 macrophages, and M2 macrophages. Representative images of (A) a PD-1 and (B) a PD-L1 staining results. (C) mIF staining results for panel 1 (CD3, CD8, FOXP3). Two images from a tumor sample showing a T helper cell ($CD3^+$, $CD8^-$, and $FOXP3^-$, light blue arrow), CTL ($CD3^+$, $CD8^+$, and $FOXP3^-$, dark blue arrow), and Treg ($CD3^+$, $CD8^-$, and $FOXP3^+$, red arrow). Scale bars = 50 µm. (D) mIF staining results for panel 2 (CD163, CD68, CD20). Two images from a tumor sample showing a B cell ($CD163^-$, $CD68^-$, and $CD20^+$, orange arrow), M1 macrophage ($CD163^-$, $CD68^+$, and $CD20^-$, yellow arrow), and M2 macrophage ($CD163^+$, $CD68^+$, and $CD20^-$, green arrow). Scale bars = 50 µm. mIF = multiplex immunofluorescence; Th = T helper cell; CTL = cytotoxic T cell; Treg = regulatory T cell.

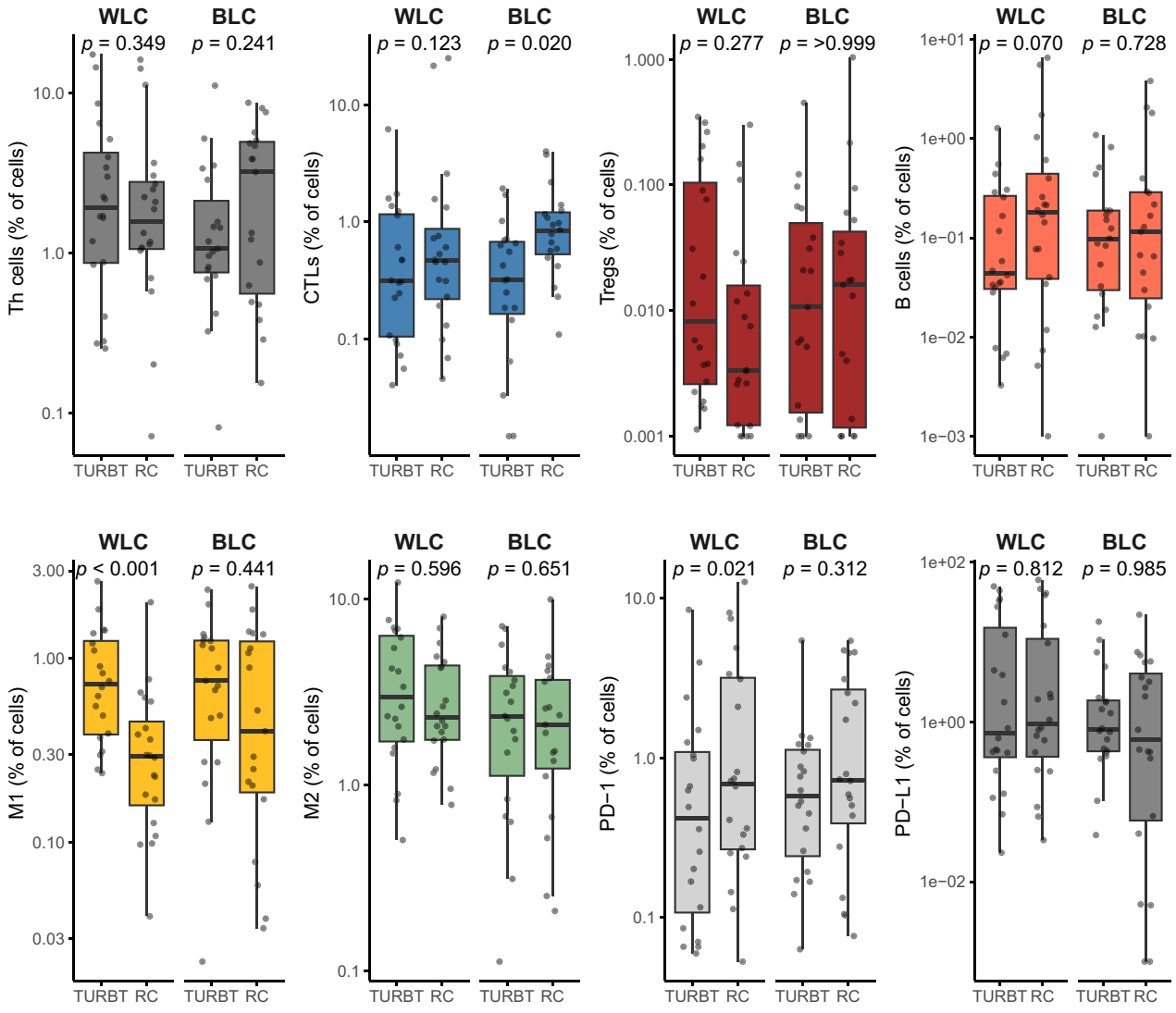

Fig. 3 – Immune cell infiltration in the carcinoma region in specimens from patients treated with either WLC- or BLC-guided TURBT. Carcinoma immune cell infiltration (Th cells, CTLs, Tregs, B cells, M1 and M2 macrophages) and immune evasion markers (PD-1, PD-L1) in TURBT and RC samples stratified by treatment group. Immune cell infiltration was defined as the percentage of total cells in the carcinoma region classified as the respective immune cell type. Immune evasion levels were defined as the percentage of total cells in the carcinoma region expressing PD-1 or PD-L1. The *y*-axes are transformed to $\log_{10}$ scale and a paired-sample Wilcoxon test was used to calculate *p* values. WLC = white light cystoscopy; BLC = blue light cystoscopy; TURBT = transurethral resection of bladder tumor; RC; radical cystectomy; Th = T helper cell; CTL = cytotoxic T cell; Treg = regulatory T cell.

cell infiltration. However, quantification of the total number of $CD3^+$ cells revealed significantly higher $CD3^+$ infiltration in the control group than in the HAL-BLC group, but similar results were not observed for either $CD4^+$ or $CD8^+$ [14]. In our study, we observed no relative changes in CTL ($CD3^+CD8^+$ cells) infiltration in carcinoma regions.

Comparison of the relative change between our WLC and BLC groups revealed a significantly lower relative proportion of stromal B cells in BLC samples. B cells are antigen-presenting cells and produce antibodies that can promote antitumor immunity. However, studies have demonstrated that B cells have both antitumor and protumor effects, depending on the phenotype and TME composition [18], so it is difficult to determine the effect of the change in stromal B-cell infiltration we observed.

Finally, we also observed a relative change in stromal PD-1 expression that was significantly lower in BLC than in WLC samples. This might reflect an increase in T-cell activity in patients who have undergone BLC-TURBT and downregulation of intratumoral T-cell activity in patients who have undergone WLC-TURBT. The effect of high PD-1 expression has been difficult to assess, as studies have reported associations with both better and worse prognosis [19]. PD-1 is a marker of T-cell exhaustion and lower expression in the stroma of BLC samples could be a sign of lower T-cell exhaustion and thus a higher antitumor immune response, indicating a treatment effect of BLC-TURBT beyond tumor detection. It could also be a result of the lower level of stromal CTLs observed in patients treated with BLC-TURBT in comparison to WLC-TURBT treatment.

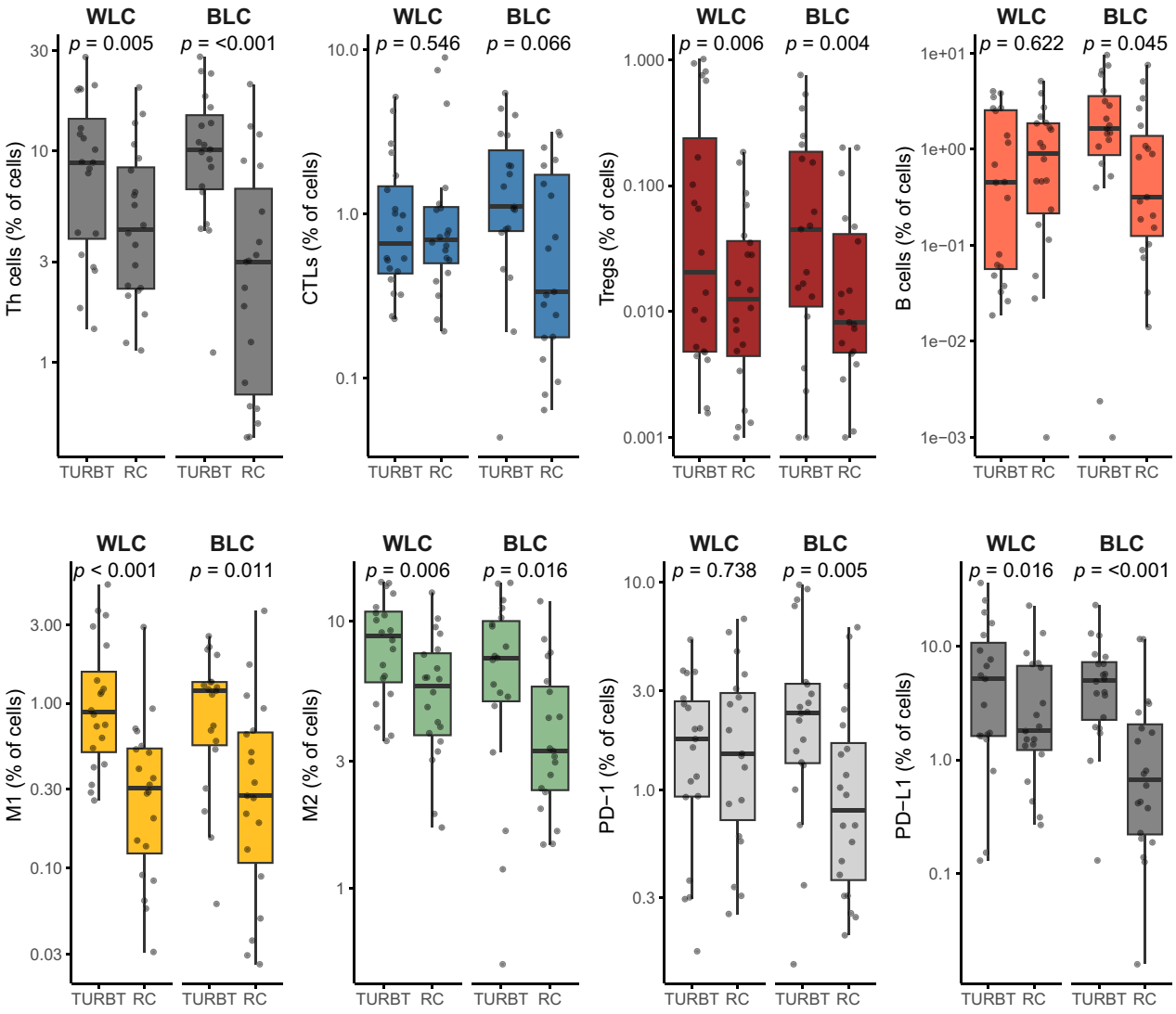

Fig. 4 – Immune cell infiltration in stromal regions in specimens from patients treated with either WLC- or BLC-guided TURBT. Stromal immune cell infiltration (Th cells, CTLs, Tregs, B cells, M1 and M2 macrophages) and immune evasion markers (PD-1, PD-L1) in TURBT and RC samples stratified by treatment group. Immune cell infiltration was defined as the percentage of total cells in the stromal region classified as the respective immune cell type. Immune evasion levels were defined as the percentage of total cells in the stromal region expressing PD-1 or PD-L1. The *y*-axes are transformed to $\log_{10}$ scale and a paired-sample Wilcoxon test was used to calculate *p* values. WLC = white light cystoscopy; BLC = blue light cystoscopy; TURBT = transurethral resection of bladder tumor; RC; radical cystectomy; Th = T helper cell; CTL = cytotoxic T cell; Treg = regulatory T cell.

Although PDD is a well-established procedure for helping to visualize tumors during TURBT, the treatment is not without limitations. It is more expensive than traditional WLC and requires prior instillation of the photosensitizer, which is not necessary in other imaging-enhanced modalities such as narrow band imaging (NBI), which is recommended as an alternative to BLC-TURBT [2,20]. Even though PDD can increase visualization of possible malignant lesions, it provides no guarantee that all lesions will be visible. Conversely, there is a risk of false positives, seen in inflamed tissue, for example [21]. BLC-TURBT might have a benefit over NBI because of its potential additional antitumor effect, whereas NBI only uses light exposure and no photosensitizer, and thus has no effect beyond tumor detection. Overall, few adverse events have been reported for the HAL-BLC procedure [22–24].

To investigate changes in the TME between TURBT and RC, we set criteria for patient selection to require the presence of tumor at the time of RC (pT1–T4a). Since it was a requirement to have residual disease at the time of RC, we did not include bladder cancer patients who had bladder pathologic complete response (<T1) as a result of TURBT. This bias might affect the results by masking the potential PDT effect of BLC-guided TURBT.

Our study is limited by the retrospective study design and the interobserver variability associated with manual

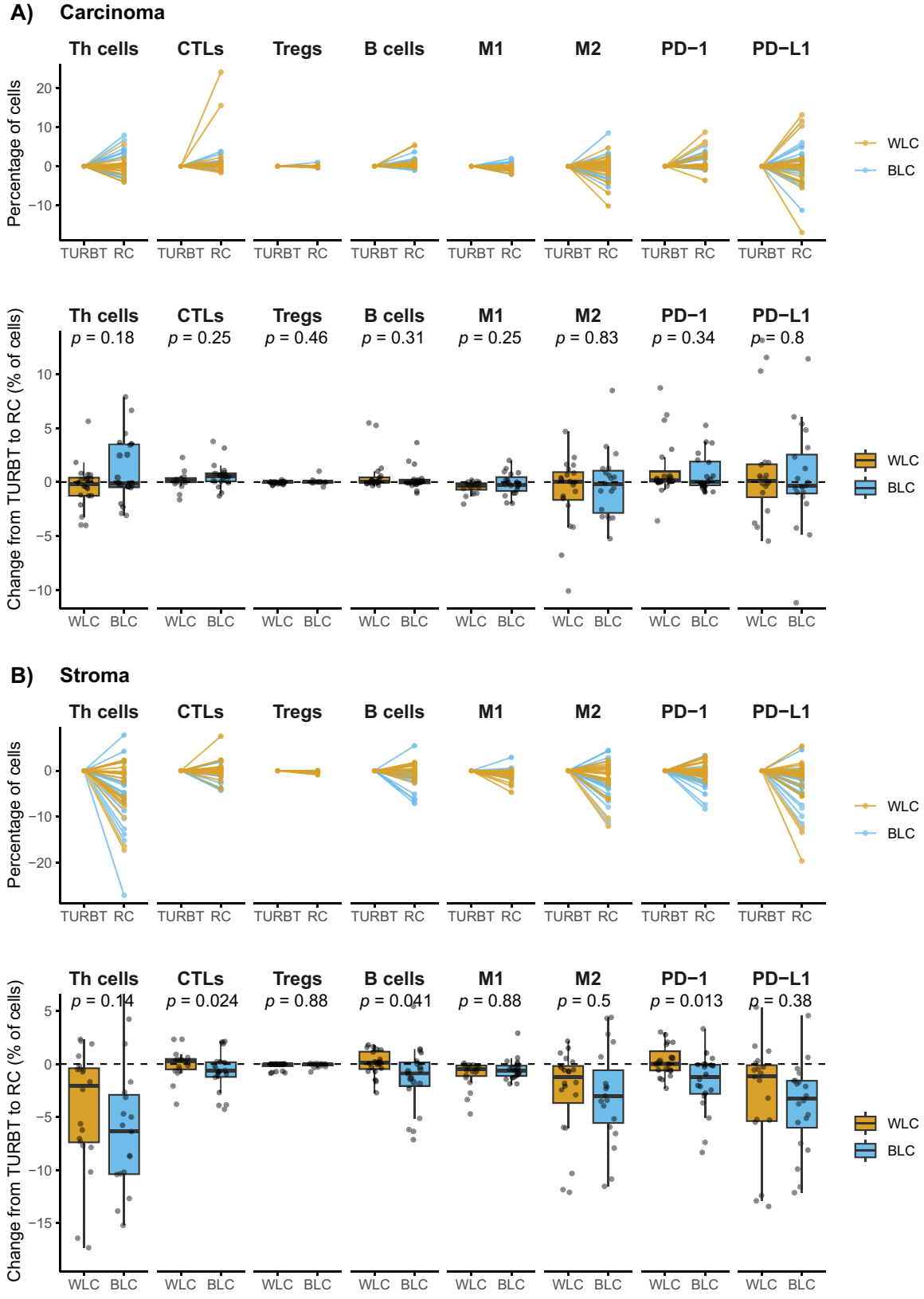

Fig. 5 – Changes in the tumor microenvironment between paired TURBT and RC samples in patients treated with WLC- or BLC-guided TURBT. Changes in the percentage of (A) intratumoral cells and (B) peritumoral cells between paired TURBT and RC samples. The Wilcoxon rank sum-test was used to calculate *p* values. WLC = white light cystoscopy; BLC = blue light cystoscopy; TURBT = transurethral resection of bladder tumor; RC; radical cystectomy; Th = T helper cell; CTL = cytotoxic T cell; Treg = regulatory T cell.

corrections in the workflow for digital image analysis. Furthermore, it should be noted that our approach does not identify which cell types expressed PD-1 and PD-L1.

5. Conclusions

Our pilot study in bladder cancer patients showed that HAL-BLC during TURBT may influence the immune cell composition and TME. Further studies are needed to verify this and elucidate whether HAL-BLC has a therapeutic role in the treatment of bladder cancer and long-term clinical effects besides guiding the cystoscopy procedure.

Author contributions: Lars Dyrskjøt had full access to all the data in the study and takes responsibility for the integrity of the data and the accuracy of the data analysis.

Study concept and design: Dyrskjøt, Taber, Young-Halvorsen, Neijber, Jensen.
Acquisition of data: Elbæk, Andreasen, Taber.
Analysis and interpretation of data: Elbæk, Andreasen, Dyrskjøt, Young-Halvorsen, Neijber.
Drafting of the manuscript: Elbæk, Andreasen, Dyrskjøt.
Critical revision of the manuscript for important intellectual content: Elbæk, Andreasen, Taber, Young-Halvorsen, Neijber, Jensen, Dyrskjøt.
Statistical analysis: Elbæk, Andreasen.
Obtaining funding: Dyrskjøt.
Administrative, technical, or material support: Jensen, Dyrskjøt.
Supervision: Dyrskjøt.
Other: None.

Financial disclosures: Lars Dyrskjøt certifies that all conflicts of interest, including specific financial interests and relationships and affiliations relevant to the subject matter or materials discussed in the manuscript (eg, employment/affiliation, grants or funding, consultancies, honoraria, stock ownership or options, expert testimony, royalties, or patents filed, received, or pending), are the following: Anders Neijber and Kristine Young-Halvorsen are employees of and hold stock or stock options in Photocure ASA. Jørgen Bjerggaard Jensen is an advisory board member for Ferring, Roche, Cepheid, Urotech, Olympus, AMBU, Janssen; Speaker: Medac, Olympus, Intuitive Surgery, and Photocure ASA; and is involved in research collaborations with Medac, Photocure ASA, Roche, Ferring, Karl Storz, Olympus, Intuitive Surgery, Astellas, Cepheid, Nucleix, Urotech, Pfizer, and AstraZeneca. Lars Dyrskjøt has sponsored research agreements with Natera, C2i Genomics, AstraZeneca, Photocure, and Ferring; has an advisory/consulting role at Ferring, MSD, and UroGen; has received speaker honoraria from AstraZeneca, Pfizer, and Roche; and is a board member for BioXpedia. The remaining authors have nothing to disclose.

***Funding/Support and role of the sponsor*:** This work was funded by a grant from Photocure ASA to Lars Dyrskjøt. The sponsor played a role in the design and conduct of the study; interpretation of the data; and review and approval of the manuscript.

Appendix A. Supplementary data

Supplementary data to this article can be found online at https://doi.org/10.1016/j.euros.2023.10.007.

References

[1] Bryan RT, Collins SI, Daykin MC, et al. Mechanisms of recurrence of Ta/T1 bladder cancer. Ann R Coll Surg Engl 2010;92:519–24.
[2] Babjuk M, Burger M, Capoun O, et al. European Association of Urology Guidelines on non–muscle-invasive bladder cancer (Ta, T1, and carcinoma in situ). Eur Urol 2022;81:75–94.
[3] Neuzillet Y, Methorst C, Schneider M, et al. Assessment of diagnostic gain with hexaminolevulinate (HAL) in the setting of newly diagnosed non–muscle-invasive bladder cancer with positive results on urine cytology. Urol Oncol 2014;32:1135–40.
[4] Geavlete B, Multescu R, Georgescu D, Jecu M, Stanescu F, Geavlete P. Treatment changes and long-term recurrence rates after hexaminolevulinate (HAL) fluorescence cystoscopy: does it really make a difference in patients with non-muscle-invasive bladder cancer (NMIBC)? BJU Int 2012;109:549–56.
[5] Stenzl A, Burger M, Fradet Y, et al. Hexaminolevulinate guided fluorescence cystoscopy reduces recurrence in patients with nonmuscle invasive bladder cancer. J Urol 2010;184:1907–13.
[6] Rink M, Babjuk M, Catto JWF, et al. Hexyl aminolevulinate-guided fluorescence cystoscopy in the diagnosis and follow-up of patients with non–muscle-invasive bladder cancer: a critical review of the current literature. Eur Urol 2013;64:624–38.
[7] Burger M, Grossman HB, Droller M, et al. Photodynamic diagnosis of non–muscle-invasive bladder cancer with hexaminolevulinate cystoscopy: a meta-analysis of detection and recurrence based on raw data. Eur Urol 2013;64:846–54.
[8] Kausch I, Sommerauer M, Montorsi F, et al. Photodynamic diagnosis in non–muscle-invasive bladder cancer: a systematic review and cumulative analysis of prospective studies. Eur Urol 2010;57:595–606.
[9] Filonenko EV, Kaprin AD, Alekseev BY, et al. 5-Aminolevulinic acid in intraoperative photodynamic therapy of bladder cancer (results of multicenter trial). Photodiagnosis Photodyn Ther 2016;16:106–9.
[10] Bader MJ, Stepp H, Beyer W, et al. Photodynamic therapy of bladder cancer – a phase I study using hexaminolevulinate (HAL). Urol Oncol 2013;31:1178–83.
[11] Lu Y, Sun W, Du J, Fan J, Peng X. Immuno-photodynamic therapy (IPDT): organic photosensitizers and their application in cancer ablation. JACS Au 2023;3L:682–99.
[12] Verger A, Brandhonneur N, Molard Y, et al. From molecules to nanovectors: current state of the art and applications of photosensitizers in photodynamic therapy. Int J Pharm 2021;604:120763.
[13] Alzeibak R, Mishchenko TA, Shilyagina NY, Balalaeva IV, Vedunova MV, Krysko DV. Targeting immunogenic cancer cell death by photodynamic therapy: past, present and future. J Immunother Cancer 2021;9:e001926.
[14] Lamy L, Thomas J, Leroux A, et al. Antitumor effect and induced immune response following exposure of hexaminolevulinate and blue light in combination with checkpoint inhibitor in an orthotopic model of rat bladder cancer. Biomedicines 2022;10:548.
[15] Taber A, Christensen E, Lamy P, et al. Molecular correlates of cisplatin-based chemotherapy response in muscle invasive bladder cancer by integrated multi-omics analysis. Nat Commun 2020;11:4858.
[16] RStudio Team. RStudio: integrated development environment for R. Boston, MA: RStudio PBC; 2022. URL. http://www.rstudio.com/.
[17] Thommen DS, Schumacher TN. T cell dysfunction in cancer. Cancer Cell 2018;33:547–62.
[18] Sharonov GV, Serebrovskaya EO, Yuzhakova DV, Britanova OV, Chudakov DM. B cells, plasma cells and antibody repertoires in the tumour microenvironment. Nat Rev Immunol 2020;20:294–307.
[19] Taber A, Prip F, Lamy P, et al. Immune contexture and differentiation features predict outcome in bladder cancer. Eur Urol Oncol 2022;5:203–13.
[20] Danske Multidisciplinære Cancer Grupper. Blærecancer. Kliniske retningslinjer. https://www.dmcg.dk/Kliniske-retningslinjer/kliniske-retningslinjer-opdelt-paa-dmcg/cancer-i-urinvejene/blaerecancer/.
[21] Draga ROP, Grimbergen MCM, Kok ET, Jonges TN, van Swol CFP, Ruud Bosch JLH. Photodynamic diagnosis (5-aminolevulinic acid) of transitional cell carcinoma after bacillus Calmette-Guérin immunotherapy and mitomycin C intravesical therapy. Eur Urol 2010;57:655–60.

[22] Pohar KS. Blue light cystoscopy: indications and outcomes. Curr Urol Rep 2020;21:19.
[23] Lotan Y, Bivalacqua TH, Downs T, et al. Blue light flexible cystoscopy with hexaminolevulinate in non-muscle-invasive bladder cancer: review of the clinical evidence and consensus statement on optimal use in the USA – update 2018. Nat Rev Urol 2019;16:377–86.
[24] Veeratterapillay R, Gravestock P, Nambiar A, et al. Time to turn on the blue lights: a systematic review and meta-analysis of photodynamic diagnosis for bladder cancer. Eur Urol Open Sci 2021;31:17–27.